Model for the Solid–Liquid Phase Transitions (Melting) of Undiluted Random Semicrystalline Copolymers of Vinylidene Chloride with Methyl Acrylate Monomers

Bernard E. Obi* and Phillip DeLassus

The Dow Chemical Company, Midland, Michigan 48667

Eric A. Grulke

Michigan State University, East Lansing, Michigan 48490

Received March 18, 1994®

ABSTRACT: A comprehensive pseudoequilibrium melting model for pure random copolymers of vinylidene chloride (VDC) with methyl acrylate (MA) monomers is developed. The model incorporates a composition-dependent surface free energy contribution to the melting point depression of these copolymers. Total exclusion of noncrystallizable copolymer units from the crystal phase is assumed for this copolymer system, and this leads to a thin lamellar crystal morphology. A physical model for these crystals is shown, and a large lateral surface area relative to the volume of the crystal is suggested. The surface to volume ratio increases with increasing copolymer composition. The model developed in this work has an excellent fit to experimental melting point data. A nonlinear composition dependence was observed for the measured melting temperatures of these copolymers, and this was well predicted by the model.

Introduction

Many crystalline polymers precipitate from their reaction medium during synthesis and form a separate phase because of more favorable polymer–polymer interactions. The precipitated polymer particles aggregate as the polymerization progresses, resulting in a finely subdivided porous resin powder. The degree of subdivision, otherwise termed granulation and generally measured by either porosity or specific surface area of the resin, is an extremely important property of these types of polymer materials. The polymer porosity or specific surface area to a large degree determines the ease of plasticizer and other additive incorporation into the polymer. More importantly, the ease of the removal of unreacted monomers and solvents used in the polymerization is determined in large part by the size of the distinct internal particles that make up the resin bead's internal microstructure morphology. Given that diffusivity for a specific monomer, solvent, or plasticizer into or out of a specific polymer at fixed conditions is nearly constant, optimization of rates of desorption of solvents and unreacted monomers and sorption of plasticizers rests solely on the particle diameter (path length).

Significant effort has been spent by several researchers in studying various aspects of monomer desorption and plasticizer absorption processes in poly(vinyl chloride) (PVC). The role of resin particle microstructure was clearly suggested. Berens[1] applied Crank's[2] work on various transport processes in polymers to the problem of residual vinyl chloride desorption in PVC resins produced by the suspension polymerization process. The work clearly demonstrated the role of the distinct internal resin particle sizes on the observed rate of monomer removal in this polymer and consequently the contribution of the internal particle dimensions to the overall efficiency in the manufacture of the polymer. Optimization of the total process time in the batch polymerization process of these resins is dependent on the time required for the recovery of unreacted monomers or solvents following the completion of the polymerization reaction.

Since the beginning of PVC resin production, there have been many attempts to understand the formation of the powder morphology. Grulke[3] and Yuan et al.[4] have reviewed the heterogeneous suspension polymerization processes in which aspects of the process that influence the resin morphology were highlighted as critical to achieving superior process and product results. Several mechanisms have been advanced over the years on the formation of grain morphology in PVC. One physical model for grain morphology formation suggests a multistage process beginning at the start of the polymerization with phase separation and going through growth and agglomeration stages as the polymerization progresses, leading to the final porous powder morphology at the end of the polymerization.[5–7] The phase-separation phenomenon in this polymer is said to result from its insolubility in its monomer. The phase-separation process is highly temperature-dependent, and therefore the choice of appropriate polymerization temperature profiles can be used to optimize the grain morphology in PVC as well as in other polymers which phase-separate from their reaction media during synthesis.

Several workers have reported work on the influence of additives on morphology formation during polymer synthesis.[8,9] The effect of temperature has been clearly suggested but in a qualitative manner. Most of the work in the literature has also dealt with homopolymers that are either amorphous with significant insolubility in their monomer (like PVC) or crystalline polymers which separate because of either liquid–liquid or liquid–solid demixing. Wessling et al.[10] have looked at the particle morphology formation processes in poly(vinylidene chloride) (PVDC). Most of the work is qualitative in nature, and inferences were drawn from this work regarding how the copolymers of vinylidene chloride would behave.

Very little work exists in the literature concerning morphology formation and control strategies in copolymers that phase-separate during polymerization. Sometimes these copolymers represent the more commercially valuable polymeric materials. The addition of comonomer changes the physical properties of the resulting copolymer

* To whom correspondence should be addressed.

® Abstract published in *Advance ACS Abstracts*, August 1, 1994.

0024-9297/94/2227-5491$04.50/0

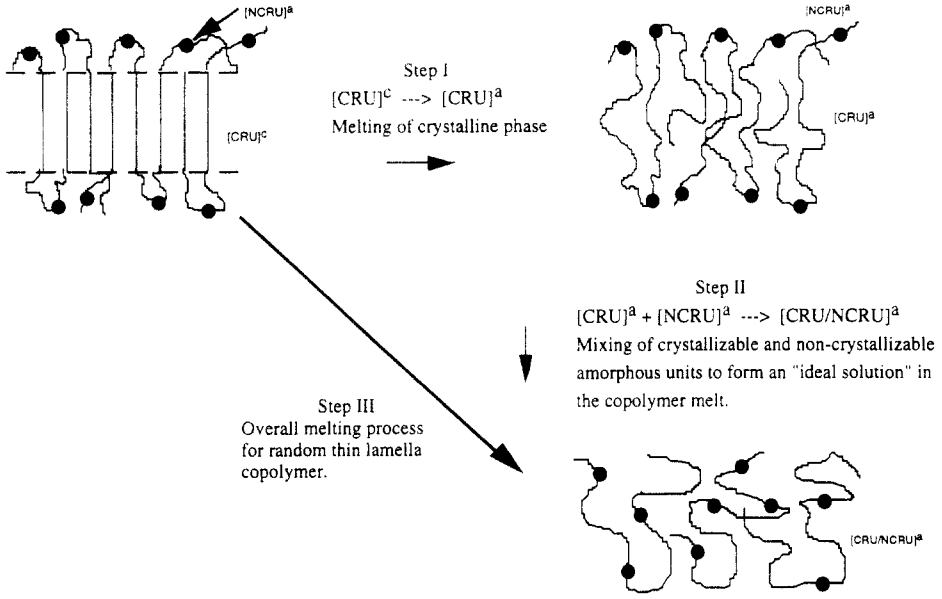

Figure 1. General schematic of the pathway for the melting/dissolution process for a semicrystalline random copolymer with noncrystallizable constitutional units. Model for thin lamellar crystals with lateral surface area. NCRU = noncrystallizable repeating units, CRU = crystallizable repeating unit. [ ]^j: j = amorphous (a) or crystalline (c) state of the phase.

in a predictable manner. The ability to control polymer resin powder morphology during synthesis requires comprehensive understanding of two main features of the heterogeneous polymerization process. Liquid–liquid (L–L) demixing and liquid–solid (L–S) demixing (crystallization) are both sources for phase separation of macromolecules from their reaction media. Loss in volume following the transformation from monomer to amorphous polymer and from amorphous polymer to crystalline polymer leads to formation of voids (porosity) in the resulting semicrystalline polymer particles. Coalescence of swollen amorphous liquid polymer droplets following L–L demixing and agglomeration of crystalline solid polymer particles following L–S demixing lead to loss of degree of subdivision or porosity in the resulting resin. The two processes mentioned above are thought to occur simultaneously with the formation of macromolecules during heterogeneous polymerization processes.

Solid–liquid (S–L) transitions, which include melting/dissolution or reorganization of macromolecule chains on precipitated particle surfaces, provide the mechanism for particle agglomeration during polymer synthesis, leading to loss of resin porosity. This paper details studies carried out by differential scanning calorimetry (DSC) to develop a model for the solid–liquid transitions (melting) of copolymers of vinylidene chloride (VDC) and methyl acrylate (MA) monomers. The pure copolymer melting model will be used to further develop the more pertinent model for copolymer melting/dissolution processes in their reaction media which can occur during polymer synthesis.

The pure copolymer melting process modeled in this work assumes the total exclusion of noncrystallizable copolymer units (MA) from the crystalline phase. Novel features of the model include a nonconstant surface free energy term and the recognition of the dependence of the surface free energy (σ) and the crystal thickness (l_c) on the copolymer composition. The copolymer melting model provides a means of evaluating the relative magnitude of the surface free energy contribution to the melting point depression as a function of copolymer composition.

Background and Theory

Many polymers are semicrystalline, in which an ordered crystalline (solid) phase coexists with a disordered molten amorphous (liquid) phase. When the temperature of the system is slowly raised, a temperature is reached at which the chemical potentials of the crystallizable unit (μ_u) in both the solid and the liquid phases are equal. This temperature is designated the equilibrium melt temperature, T_m. If the polymer is a one-component system, otherwise known as a homopolymer, then T_m is designated $T_m°$. A mathematical description of the above statement by Flory[11] is shown in eq 1, where μ_u^c represents the chemical potential of the crystallizable unit (u) in the crystalline (solid) phase and $\mu_u°$ represents its chemical potential in the standard state, which is the pure amorphous polymer melt "liquid" at $T_m°$ and the prevailing ambient pressure.

$$[\mu_u^c - \mu_u°] \equiv \Delta\mu_u^c = 0, \quad \text{at } T_m° \tag{1}$$

When a diluent in the form of copolymer units is present in the polymer, the chemical potential of the crystallizable unit in the amorphous copolymer melt (liquid) phase, μ_u^{cop}, is less than $\mu_u°$. Thus to reestablish the condition of equilibrium, ($\mu_u^{cop} = \mu_u^c$), a new equilibrium temperature, T_m^{cop}, is required. The new equilibrium temperature T_m^{cop} is usually less than $T_m°$. The conditions of equilibrium between the crystallizable polymer unit in the crystal (solid) phase and the same in the amorphous (liquid) phase can be mathematically restated as

$$[\mu_u^c - \mu_u°] = [\mu_u^{cop} - \mu_u°] \equiv \Delta\mu_u^c = \Delta\mu_u^{cop}, \quad \text{at } T_m^{cop} \tag{2}$$

where eq 2 describes the equality between the differences in the chemical potentials for the crystallizable repeating unit in the crystal and copolymer "dilute" amorphous phases relative to the standard state at the new equilibrium temperature T_m^{cop}.

Figure 1 is a schematic of a physical model showing the thermodynamic pathway of the copolymer melting process. From Figure 1 we see that step I followed by step II, or step III alone, yields the same change in state. The change in chemical potential associated with step I and shown in eq 2 as $\Delta\mu_u^c$ is equal to the overall free energy change for the fusion (melting) process of the crystalline phase of the

semicrystalline copolymer.

$$\Delta\mu_u^c = -\Delta G_f$$

where ΔG_f is the overall free energy of fusion (3)

$$\Delta G_f = \Delta g_b - \left(\frac{10M_u^\circ}{\rho_c}\right)\frac{2\sigma}{l_c} \quad (4)$$

where Δg_b is the bulk free energy of fusion, σ is the surface free energy, and l_c is the average lamella thickness. The term $10M_u^\circ/\rho_c$ is a conversion factor to transform erg/cm^2-Å to J/mol. The bulk free energy of fusion is written as

$$\Delta g_b = \Delta H_u\left(1 - \frac{T_m^{cop}}{T_m^\circ}\right) \quad (5)$$

where ΔH_u is the heat of fusion for a hypothetical 100% crystalline PVDC homopolymer. Finally, the change in the chemical potential term of the crystallizable units in the crystalline phase is written for the case of total exclusion of noncrystallizable copolymer units from the crystal as

$$\Delta\mu_u^c = -\Delta G_f = -\left(\Delta H_u\left(1 - \frac{T_m^{cop}}{T_m^\circ}\right) - \frac{20M_u^\circ\sigma}{\rho_c l_c}\right) \quad (6)$$

The chemical potential of the crystallizable unit in the copolymer melt given as $\Delta\mu_u^{cop}$ in eq 2 can be rewritten in more measurable terms as

$$\Delta\mu_u^{cop} = RT_m^{cop}\ln(a_u^{cop}) \equiv RT_m^{cop}\ln(\gamma_u^{cop}X_u^{cop}) \quad (7)$$

where a_u^{cop} is the activity of the crystallizable units in the copolymer melt solution, γ_u^{cop} is the activity coefficient, and X_u^{cop} is the mole fraction of the crystallizable units in the copolymer mixture. For a perfectly random copolymer, an ideal mixture approximation can be applied. Then the activity coefficient is approximately unity, and eq 7 simplifies to eq 8.

$$\Delta\mu_u^{cop} = RT_m^{cop}\ln(X_u^{cop}) \quad (8)$$

When eq 2 is rewritten in terms of measurable quantities, the melting point equation for pure random copolymers becomes

$$\Delta H_u\left(1 - \frac{T_m^{cop}}{T_m^\circ}\right) - \frac{20M_u^\circ\sigma}{\rho_c l_c} = -RT_m^{cop}\ln(X_u^{cop}) \quad (9)$$

Further rearrangements of eq 9 give melt transition temperature equations for pure random copolymers as eqs 10 and 11.

$$\frac{1}{T_m^{cop}}\left(1 - \frac{20M_u^\circ\sigma}{\Delta H_u\rho_c l_c}\right) - \frac{1}{T_m^\circ} = -\frac{R}{\Delta H_u}\ln(X_u^{cop}) \quad (10)$$

$$\frac{1}{T_m^{cop}} = \frac{1}{T_m^\circ\left(1 - \frac{20M_u^\circ\sigma}{\Delta H_u\rho_c l_c}\right)} - \frac{R}{\Delta H_u\left(1 - \frac{20M_u^\circ\sigma}{\Delta H_u\rho_c l_c}\right)}\ln(X_u^{cop}) \quad (11)$$

In eqs 10 and 11 T_m^{cop} is the melt temperature of the pure copolymer, X_u^{cop} is the mole fraction of the crystallizable units in the copolymer, R is the universal gas constant, ΔH_u is the heat of fusion per mole of crystallizable repeat units based on 100% crystallinity (J/mol), ρ_c is the density of the pure 100% crystal (g/cm^3), M_u° is the formula weight of the crystallizable monomeric unit (g/mol), σ is the end surface free energy of the crystal lamella (erg/cm^2), and l_c is the crystal lamella thickness (Å).

Experimental Section

Copolymer Resin Preparation. Reagent grades of distilled vinylidene chloride monomer from The Dow Chemical Co. and methyl acrylate monomer with 200 ppm MEHQ (monomethyl ether of hydroquinone) from Aldrich Chemical Co. were sparged with nitrogen gas to eliminate oxygen. An appropriate peroxide radical polymerization initiator was mixed with each monomer separately. From the two solutions, five compositions of VDC–MA mixtures were made up to produce 0.0, 4.0, 8.0, 12.0, and 16.0 wt % MA copolymers.

An appropriate time and temperature profile was designed to yield copolymers with a number-average molecular weight (M_n) of approximately 45 000 (equivalent 450+ monomer units per macromolecule). A suspension solution of 0.15 wt % Methocel cellulose ether from The Dow Chemical Co. was prepared in deionized water.

For each composition, 100 g of the monomer mixture was added to 150 g of the suspension solution in polymerization reaction bottles. The bottles were then shaken for 30 min to disperse the monomer/initiator (oil phase) into tiny droplets. The dispersion of the oil phase into droplets of about 500 μm was to ensure adequate heat transfer from the reaction vessel and good temperature control. The five bottles were loaded into a Bendix polymerizer, which is a well-controlled temperature bath with agitation capability. The reaction mixtures were subjected to the time–temperature profile to ensure about 95% conversion of monomer to polymer and a number-average molecular weight (M_n) of about 45 000.

At the end of the polymerization reaction, the resins were washed several times with cold deionized water. The resins were then filtered and dried in an oven at 85 °C for 24 h. This treatment is required to remove moisture and unreacted monomers from the resins.

Characterization of Copolymer Resins. Conflicting data exist regarding the equilibrium heat of fusion, ΔH_u, of the PVDC homopolymer. The values generally found in the literature range from about 62 to 74 J/g.[21-23] We suspect the true value for ΔH_u is higher than those reported in the literature. Copolymers separately prepared in the manner discussed above and covering a broader range of composition were previously prepared. The heats of fusion of the nascent (as polymerized) copolymer resins were measured by differential scanning calorimetry (DSC) on all the samples prepared. The heats of fusion were obtained using the Dupont 9900 calorimeter. Approximately 10 mg of sample was placed in an aluminum pan and sealed. The reference cell had an empty aluminum pan. A heating rate of 10 °C min^{-1} was used for all the scans. The total area under the endotherm was used to evaluate the heats of fusion.

The densities of these copolymer samples were measured by a helium pycnometry method using the Accupyc 1330 pycnometer from Micromeritics Instruments Corp. This method accurately measures the true volume of a given sample by completely filling the space around it with a known volume of helium at a fixed temperature. The device has dual interconnected chambers C1 and C2 separated by a valve. C1 is for pure helium only, and C2 is the sample chamber. From a calibration run in the absence of sample in C2, the chamber volume V_2 is measured. A dry resin sample of accurately known mass (with precision to 10^{-6} g) is then placed in C2 and a known amount of helium at a pressure P_1 is placed in C1. The valve is opened and after equilibration the final pressure P_2 of the helium in the system is read. Application of the following equation is used to determine the volume of the sample. $P_1V_1 = P_2(V_1 + V_2 - V_s)$. Since values for all variables are known except for V_s, which is the sample volume, V_s is obtained. The true, otherwise known as skeletal, density or the true specific volume of the copolymer sample is then calculated using the sample mass and V_s. The densities measured by this technique are accurate to the third decimal place. The specific volumes measured for these samples were plotted as a function of the copolymer composition. The data

Table 1. Measured Physical Properties of VDC–MA Copolymers

copolym comp (wt % MA)	exptl heat of fusion (J/g)	measd density (g/cm^3)	calcd amorph density (g/cm^3)	fract cryst (α_c)	normalized heat of fusion (α_c = 1.0) (J/g)
		(1.960)[a]	(1.767)[b]	(1.00)	(95.556)[c]
0.0	56.530	1.873	1.767	0.5774	97.904
1.20	53.050	1.860	1.754	0.5435	97.608
2.10	51.830	1.849	1.746	0.5120	101.23
4.20	41.750	1.828	1.726	0.4671	89.381
6.70	35.970	1.797	1.702	0.4011	89.678
8.10	33.600	1.779	1.690	0.3630	92.562
10.0	24.410	1.735	1.674	0.2437	100.16
12.0	17.210	1.696	1.656	0.1520	113.22
14.0	9.368	1.672	1.639	0.1197	78.260
16.0	ND[d]	1.643	1.623		
18.0	ND	1.621	1.607		
20.1	ND	1.615	1.591		
30.0	ND	1.511	1.519		
50.0	ND	1.433	1.297		
80.1	ND	1.251	1.253		
100	ND	1.178	1.178		

[a] Based on the unit cell dimension of PVDC. [b] Extrapolated from specific volume versus composition (percent MA in copolymer). [d] ND = not detected.

fell into two distinct linear regions. A linear fit of the amorphous region was interpolated back to the pure homopolymer composition from which the specific volume and hence the density of the pure amorphous homopolymer was obtained; see Table 1. The value obtained in this work is consistent with that obtained by previous researchers for this copolymer system.[22] The 100% crystalline density of the homopolymer (PVDC) is known using the unit cell dimensions;[22] see Table 1 also. The specific volumes of pure poly(methyl acrylate) and that of pure poly(vinylidene chloride) together with a weighting method were used to obtain the specific volumes of the copolymers for each composition. Knowing the specific volumes for the pure crystalline and amorphous states for the copolymers allowed the level of crystallinity in the samples to be calculated by the volume method: $\alpha_c(x) = (v_x - v_{xa})/(v_c - v_{xa})$, where $\alpha_c(x)$ is the fractional crystallinity for the copolymer of composition x, v_x is the specific volume of the semicrystalline copolymer sample, v_{xa} is the specific volume of the totally amorphous copolymer, and v_c is the specific volume of the 100% crystalline pure homopolymer, all at 21 °C.

The measured heats of fusion for the copolymer samples were then normalized assuming a 100% crystalline copolymer. Table 1 shows data from these measurements. From Table 1, we see that a new and more likely value for the equilibrium heat of fusion for the homopolymer based on 100% crystallinity is 95.5 J/g (9263.5 J/mol of VDC units). The observed equilibrium melt temperature $T_m°$ is consistent with previous values of about 210 °C.[21] From the values of ΔH_u and $T_m°$, a new value for the entropy of fusion can be calculated as $\Delta H_u/T_m° = \Delta S_u$ with a value of 19.2 J/mol-K (4.58 cal/mol-K).

Determination of S–L Transition (Melting) Temperatures of Copolymers. Experiments were carried out by DSC using the Dupont 9900 calorimeter. Two heating rates of 5 and 10 °C min^{-1} were initially used to establish the maximum allowable equilibrium heat-up rate for the experiments. A heating rate of 10 °C min^{-1} was found to be adequate to produce thermograms without significant rate effects. The experiments were performed by placing approximately 10 mg of the copolymers into 20 μL NMR spherical glass ampules from the Wilmad Glass Co. The ampules were sealed using a propane/oxygen torch with the sample held near −70 °C under a nitrogen purge. The sealed ampules were reweighed and the weight of the copolymer was obtained by difference. A sealed empty glass ampule was used in the reference cell, and the glass ampule was used for the indium and decane calibrations to obtain the cell constants.

Results and Discussion

Figure 2 is the thermogram of an 8 wt % MA copolymer.

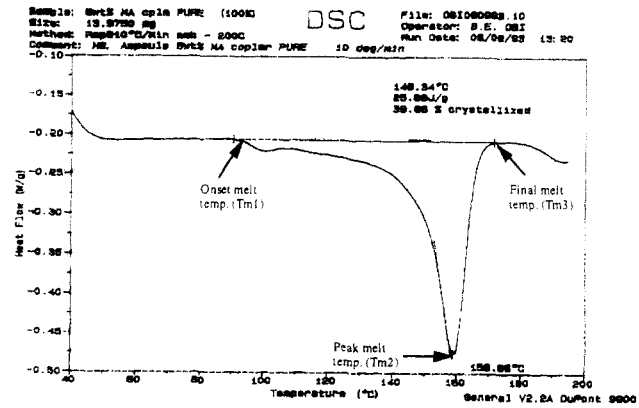

Figure 2. DSC thermogram of an 8 wt % MA–VDC copolymer resin showing various important melt transition points.

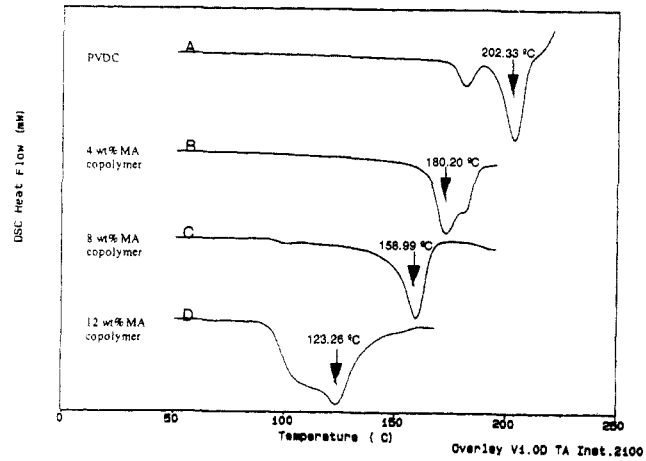

Figure 3. Overlay of the DSC scans for the four polymer samples studied in this work showing the relative positions of the onset, peak, and final melt temperatures (peak melt temperature identified).

Clearly, a very long tail precedes the peak melt temperature. This tail shows melting from about 90 °C, with the peak melting point at about 159 °C. For a slow crystallizing polymer this broad melting transition is indicative of a broad distribution of crystallite sizes, not necessarily of melting, recrystallization/annealing, and further melting during the scan.

Figure 3 shows an overlay of the thermograms for the four copolymer compositions studied in this work. There are several important features in these graphs. We find a distinct bimodal character for the more crystalline polymers, (A) PVDC homopolymer and (B) 4 wt % MA copolymer samples. As for the less crystalline, higher MA level copolymer samples C and D, significantly broader melt transition temperatures are observed. As was discussed in the paragraph above, a broad melt transition temperature is most likely indicative of a broad distribution of crystallite sizes in the nascent copolymer samples. On heating these samples, the smallest lamellar crystals melt first (lowest melt temperature), while the largest lamellar crystals melt last (highest melt temperature). The peak melt temperature is indicative of the temperature at which most of the crystals in the sample have melted. The final melt temperature is indicative of the melting of the "equilibrium" size (the largest size) lamellar crystals in the copolymer.

Table 2 contains data for the various transitions observed in the thermograms for the four compositions studied in the present work. As depicted in the thermogram of the 8 wt % MA copolymer sample (Figure 2), we designate T_{m1} as the onset melt temperature. The peak temperature

Table 2. Data of Important Transitions Occurring during Heat-up of Nascent Pure Copolymer Resins

copolym comp (wt % MA)	onset melt temp T_{m1} (°C)	peak melt temp T_{m2} (°C)	final melt temp T_{m3} (°C)
0.0	172.05	202.33	209.44
4.0	157.42	180.20	188.89
8.0	92.47	158.99	166.91
12.0	89.92	123.26	159.38
16.0	ND[a]	ND	ND

[a] ND = not detected.

Table 3. Summary Data of Important Melting Transitions Occurring during Heat-up of Nascent Pure copolymer Resins

copolym comp (wt % MA)	onset melt temp T_{m1} (°C)	peak melt temp T_{m2} (°C)	final melt temp T_{m3} (°C)	calcd Flory melt temp T_m(Flory) (°C)
0.0	173.45	200.77	204.20	210.00
0.0	172.05	202.33	209.44	210.00
1.24	170.26	194.86	199.37	207.07
2.09	169.04	192.39	197.99	205.07
4.0	157.43	180.20	188.89	200.57
4.23	161.89	178.58	183.21	200.03
6.73	91.58	163.64	169.32	194.15
8.0	92.47	158.99	166.91	191.17
8.06	90.80	159.64	163.85	191.03
9.97	90.72	154.00	160.53	186.55
12.0	89.92	123.26	159.38	181.72
12.03	88.18	122.22	144.94	181.72
14.03	91.27	118.55	123.24	177.00
16.0	ND[a]	ND	ND	172.50

[a] ND = not detected.

is designated T_{m2}. For broadly melting polymers, T_{m2} is generally considered the true melt temperature in the polymer thermal analysis literature. It is the temperature at which the majority of the crystals undergo the melt transition. T_{m3} is the final melt temperature. It is the final inflection point in the thermogram and represents the melting of the largest ("equilibrium") crystals present in the copolymer sample.

Data Analysis and Development of Appropriate Copolymer Model. Data analysis was performed using the SIMUSOLV modeling and simulation software developed at The Dow Chemical Co. The first analysis was to compare our experimental data to that predicted from the ideal copolymer equilibrium melting equation of Flory. For this analysis, the final melt temperature T_{m3} in Tables 3 was used as the "equilibrium" melt temperature for comparison with calculated values from the Flory equation. As can be seen in Table 3, the ideal copolymer equation of Flory overestimates the "equilibrium" melt temperatures of the VDC–MA copolymer system.

An assumption in the Flory model is that equilibrium crystals are treated. Equilibrium crystals imply very large or extended chain crystals. It will be impossible to meet the condition of extended chain crystals for copolymers in which one of the copolymer units is noncrystallizable as is the case in the VDC–MA system. This is particularly the case when the noncrystallizable units are predominantly excluded from the crystal. We know that the VDC–MA system is a random copolymer system in which the MA comonomer units in the copolymer backbone are noncrystallizable. The crystalline morphology is predominantly that of chain folding, and we believe that a large fraction of the MA units in the copolymer sample is rejected from the crystal and deposited at the fold surface, which is the interfacial layer adjoining the amorphous and the crystalline phases. The results of predominantly excluded noncrystallizable copolymer units from the

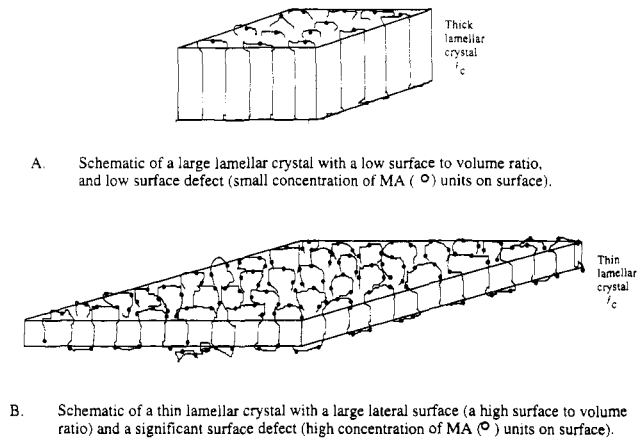

A. Schematic of a large lamellar crystal with a low surface to volume ratio, and low surface defect (small concentration of MA (○) units on surface).

B. Schematic of a thin lamellar crystal with a large lateral surface (a high surface to volume ratio) and a significant surface defect (high concentration of MA (○) units on surface).

Figure 4. Schematic showing two extreme types of lamellar crystals possible in the VDC–MA random semicrystalline copolymers.

crystal is the formation of thin lamellar crystals with large surface area.

The melting of a thin lamellar crystal with a large surface area will involve a significant surface free energy contribution to the melting point depression. Figure 4 is a schematic illustration of our view of the types of lamellar crystals present in the VDC–MA copolymer system. In looking at types A and B crystals in the illustration, we see that two important crystal parameters will be variables for this copolymer system, namely, the crystal lamellar thickness l_c and the crystal surface free energy σ. In looking at type A, we see that the surface to volume ratio is small. On the contrary, type B crystals will have a large surface to volume ratio, implying a significant surface contribution to the stability of such a thin lamellar crystal. Another important consideration in evaluating the surface energy contribution to the stability of type B crystal lamellar morphology has to do with the fact that the higher concentration of the noncrystallizable MA units at the crystal surface changes the physical structure of the chain folds at the lamellar surfaces as well as the chemical composition of the interfacial surface. Both of these will lead to an increased surface free energy with increasing copolymer composition in the noncrystallizing MA unit. The result of such increased surface free energy will be an even higher melting point depression than would be predictable using simpler ideal random copolymer melting models.

Many previous workers on polymer melting have identified the fact that the surface of thin lamellar crystals affects the melting point of such crystals. Eby and Sanchez[12] and also Bluhm, Orts, and Marchessault[13,14] investigated the melting of copolymer systems in which both copolymer units are crystallizable. In their model for the copolymer melting process, they assumed total inclusion of copolymer units in the crystal; hence lamellar thickness is not a variable. As a consequence of total inclusion of copolymer units resulting in thick lamellar crystals, melting point depression for this system is attributable not to the surface free energy contribution but to a defect energy term associated with the packing of nonisomorphic copolymer units within the crystal. On the other hand, Gilmer, Sadler, and Goldbeck-Wood,[15–19] looked at the melting processes in copolymer systems in which total exclusion of noncrystallizable copolymer units from the crystal phase was assumed. Their model was based on kinetic factors governing the crystallization process which leads to the formation of a broad distribution of nonequilibrium size crystals. The model recognizes and

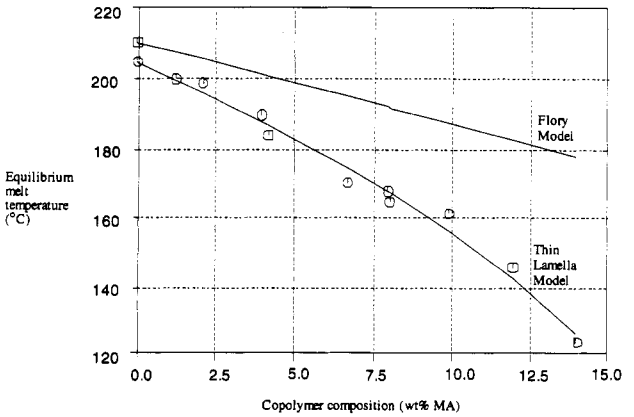

Figure 5. Graph of results from the simulation comparing the equilibrium melt temperature from the Flory model to the experimental data and the authors' thin lamella model.

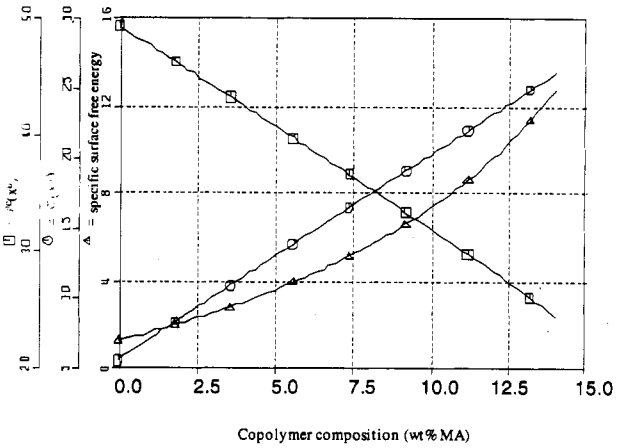

Figure 6. Graph showing the dependence of calculated lamellar thickness and surface free energy on the copolymer composition.

incorporates lamellar thickness dependence on the melting point depression of copolymers with noncrystallizable units rejected exclusively into the amorphous phase. The model defines a constant lamellar thickness parameter, l_m, which is used to fit the copolymer melting data.

Our model recognizes two main points mentioned above, which are the composition dependence of both the lamellar thickness (l_c) and surface free energy (σ). As such, eq 11 is recast below with composition-dependent surface free energies and crystal lamellar sizes.

$$\frac{1}{T_m^{cop}} = \frac{1}{T_m^\circ\left(1 - \frac{20M_u^\circ\sigma(x_u)}{\Delta H_u \rho_c l_c(x_u)}\right)} - \frac{R}{\Delta H_u\left(1 - \frac{20M_u^\circ\sigma(x_u)}{\Delta H_u \rho_c l_c(x_u)}\right)} \ln(X_u^{cop}) \quad (12)$$

Work by Landes et al.[20] on the crystal lamellar thickness of copolymers of the VDC–MA system shows an observed increasing overall lamellar thickness with increasing copolymer composition. However, when corrected for the level of crystallinity, the calculated actual crystal lamellar thickness decreased with composition as would be expected. From their data we find a logarithmic dependence of lamellar thickness l_c with copolymer composition x_u such that eq 13 is the relative lamellar size equation for copolymers of VDC–MA system.

$$l_c(x_u) = l_{c1} + \beta \ln(X_u^{cop}) \quad (13)$$

In eq 13, l_{c1} and β are adjustable parameters which are easily and independently obtainable from X-ray diffraction measurements. Substitution of appropriate values of l_{c1} (49.18 Å) and β (146.69 Å) into eq 12 leaves only the surface energy function to be determined from melting point data. In eqs 12 and 13, x_u and X_u^{cop} are used interchangeably for copolymer composition.

A relatively simple linear model was used as a first approximation for the surface free energy function for these copolymers. We had stated earlier that the surface free energy cannot be a constant because the interfacial region changes with changes in copolymer composition as illustrated in Figure 5. The rejection of the noncrystallizable (MA) units into the interfacial region concentrates the MA units at this interface, changing both its chemical and physical nature. We believe that the dissimilarity between the crystal and amorphous layers will increase with increasing MA concentration in the copolymer,

Table 4. Summary of Simulation Results Showing Observed versus Calculated Copolymer Final Melt Temperatures ($T_m3 = T_m^{cop}$), with Estimates of Surface Energy Parameters (σ_1 and α)

description	parameter estimates: initial	parameter estimates: final	standard deviation
log(likelihood function)	−50.816	−26.890	
σ_1 (ergs/cm^2)	1.0000	5.4703	1.28
α (ergs/cm^2)	1.0000	132.32	12.4

copolym comp (wt % MA)	T_m^{cop} (°C) obsd	T_m^{cop} (°C) pred	standardized % error	standardized residual	residual plot
0.000	204.2	204.3	−0.03	−0.022	|
1.240	199.4	199.1	0.13	0.093	|
2.090	198.0	195.5	1.27	0.900	| ****
4.000	188.9	187.0	1.01	0.687	| ***
4.230	183.2	185.9	−1.48	−0.970	**** |
6.730	169.3	173.7	−2.61	−1.580	******* |
8.000	166.9	167.0	−0.06	−0.033	|
8.060	163.9	166.7	−1.72	−1.010	**** |
9.970	160.5	155.6	3.10	1.780	| *******
12.03	144.9	141.8	2.18	1.130	| *****
14.04	123.2	125.7	−1.98	−0.873	**** |

causing the surface free energy to increase. Equation 14

$$\sigma(x_u) = \sigma_1 + \alpha(1 - X_u^{cop}) \quad (14)$$

is the first simple approximation to the surface free energy model as a function of the copolymer composition, where σ_1 and α are adjustable parameters necessary to describe the surface free energy dependence on the copolymer composition. Here, σ_1 represents the surface free energy of the homopolymer. These two parameters are all that is required by the model to describe the overall melting point depression for a random semicrystalline copolymer.

Figures 5 and 6 and Tables 4 and 5 contain results from simulations and data analysis using the SIMUSOLV software. From Figure 5, we see that our random copolymer model with variable surface energy contribution adequately describes the observed final (equilibrium) melt temperature for the copolymers of the VDC–MA system. There is a definite curvature (nonlinear nature) to the melt temperatures of VDC–MA copolymers as a function of composition. At higher MA levels in the copolymer, the melting point depression is greater. The variable surface energy term in the model provides the means by which this nonlinear melting point depression relationship with composition is adequately described by our model. Figure 6 is a plot of calculated values of lamellar thicknesses and the surface free energies. The exponential increase

Table 5. Results Comparing the Final Melt Temperatures Calculated from the Flory Equilibrium Model versus That of the Authors' Thin Lamella Total Exclusion Model and Calculated Values of the Lamella Sizes and Surface Free Energies

copolym comp (wt % MA)	Flory model T_m(Flory) (°C)	authors' model T_m^{cop} (°C)	lamella thickness $l_c(x_u)$ (Å)	surface free energy $\sigma(x_u)$ (ergs/cm^2)	specific surface free energy (J/g)
0.0	210.0	204.26	49.20	5.47	1.18
1.24	207.07	199.11	47.14	7.32	1.67
2.09	205.07	195.48	45.71	8.58	2.02
4.00	200.57	186.98	42.46	11.41	2.95
4.23	200.03	185.91	42.07	11.75	3.07
6.73	194.15	173.74	37.73	15.43	4.58
8.00	191.17	167.00	35.48	17.29	5.52
8.06	191.03	166.67	35.37	17.37	5.57
9.97	186.55	155.55	31.94	20.16	7.27
12.03	181.72	141.78	28.16	23.15	9.63
14.04	177.00	125.68	24.40	26.05	12.73

in specific surface energy with composition strongly suggests the role of surface energy on crystal stability and the resulting melting point depression for this copolymer system.

Table 4 shows results from the simulations to fit the experimentally observed melt temperature data. We see that the observed melt temperature compares very well with the predicted values. The very small differences between the observed and calculated melt temperatures in the error column show quantitatively how well the authors' copolymer melting model describes the melting process in the VDC–MA random semicrystalline copolymer system. Similarly, the residual scatter plot in Table 4 shows very good randomization of the error in the calculated values, which qualitatively confirms the conclusion that the model describes the melting process for this system well.

Table 5 is a summary of calculated values from the fitted model. The table shows a comparison of the final (equilibrium) melt temperature calculated by our model to that calculated from the Flory equilibrium model. We see that the Flory equilibrium model overpredicts the actual melt temperatures. Table 5 also contains calculated values of the lamellar sizes and the surface free energies as a function of copolymer composition. The last column of Table 5 contains calculated values of the specific surface energies as a function of composition. Comparison of the specific surface energies with the equilibrium heat of fusion ΔH_u gives an indication of the relative magnitude of the surface defect contribution to the melting point depression for this family of copolymers. The calculated values clearly show that as the noncrystallizable copolymer fraction increases, the surface defect contribution increases as would be expected.

Conclusions

We have developed an appropriate model to describe the "equilibrium" melting process for vinylidene chloride (VDC)-methyl acrylate (MA) semicrystalline random copolymers. The unique feature of this model is the recognition of the nonlinear nature of the equilibrium melt temperatures and, consequently, the realization that the surface free energy contribution to the melting point depression is not a constant but varies with the copolymer composition. The model—eqs 12, 13, and 14—shows good fit of the melting point data and provides a means of evaluating the surface free energies of the copolymer crystal surfaces as a function of composition. The surface to volume ratio of the crystals of this family of copolymers increases with increasing copolymer composition, and consequently the melting point depression correspondingly increases. It is generally accepted that for this copolymer system total exclusion of the noncrystallizable MA units from the crystal is the preferred crystal morphology. As such our model deliberately ignores incorporating a term for a defect energy which would arise from the inclusion of the copolymer units into the crystal when these units are nonisomorphic. If the true crystal morphology had mixed inclusion and exclusion of the noncrystallizable copolymer units, then the total defect energy required in this model to fit the data would not come from surface effects alone but would also be due to defects from the poor packing associated with the inclusion of the nonisomorphic units. The development of this pure copolymer melting model is the first step in our attempt toward development of a comprehensive generalized model for the melting/dissolution process of these copolymers in their reaction media. We believe that this model can be usefully applied to other random semicrystalline copolymer systems to predict the melting process as well as to obtain surface free energy values for the copolymers.

Acknowledgment. We gratefully acknowledge the generous assistance of Professor Carl Lira of the Department of Chemical Engineering, Michigan State University, for valuable counsel in clarifying basic thermodynamic principles. Similarly frequent discussions with Dr. Donald Kirkpatrick of The Dow Chemical Co. on the nature of the assumptions in developing the copolymer model are gratefully appreciated. Finally we thank The Dow Chemical Co. for support.

References and Notes

(1) Berens, A. R. *J. Vinyl Technol.* **1979**, *1*, 1.
(2) Crank, J. *The Mathematics of Diffusion*, 2nd ed.; Oxford University Press: Oxford, 1979.
(3) Grulke, E. A. *Encyclopedia of Polymer Science and Engineering* **1985**, *16*, 443.
(4) Yuan, H. G.; Kalfas, G.; Ray, W. H. *J. Macromol. Sci., Rev. Macromol. Chem. Phys.* **1991**, *C31* (2&3), 215.
(5) Rance, D. G.; Zichy, E. L. *Pure Appl. Chem.* **1981**, *35*, 377.
(6) Tornell, B.; Uustalu, J. *J. Appl. Polym. Sci.* **1988**, *35*, 63.
(7) Smallwood, P. V. *Polymer* **1986**, *27*, 1609.
(8) Nilsson, H.; Silvegren, C.; Tornell, B. *J. Vinyl Technol.* **1985**, *7*, 3.
(9) Tornell, B. E.; Uustalu, J. M. *J. Vinyl Technol.* **1982**, *4*, 2.
(10) Wessling, R. A.; Harrison, I. R. *J. Polym. Sci., Polym. Phys. Ed.* **1971**, *11*, 3471.
(11) Flory, P. J. *Principles of Polymer Chemistry*, 9th ed.; Cornell University Press: Ithaca, NY, 1975.
(12) Sanchez, I. C.; Eby, R. K. *Macromolecules* **1975**, *8*, 638.
(13) Orts, W. J.; Marchessault, R. H. *Macromolecules* **1991**, *24*, 6435.
(14) Bluhm, T. L.; Orts, W. J.; Marchessault, R. H. *Adv. X-Ray Anal.* **1992**, *35*, 645.
(15) Sadler, D. M.; Gilmer, G. H. *Phys. Rev. Lett.* **1986**, *56*, 25.
(16) Sadler, D. M.; Gilmer, G. H. *Phys. Rev. B* **1988**, *38*, 8.
(17) Goldbeck-Wood, G.; Sadler, D. M. *Polym. Commun.* **1990**, *31*, 143.
(18) Goldbeck-Wood, G. *Polymer* **1990**, *31*, 586.
(19) Goldbeck-Wood, G. *Polymer* **1992**, *33*, 778.
(20) Landes, B. G.; DeLassus, P. T.; Harrison, I. R. *J. Macromol. Sci., Phys.* **1983–1984**, *B22* (5&6), 735.
(21) Wessling, R. A. *Poly Vinylidene Chloride*; Gordon and Breach Science Publishers: London, 1977; Vol. 5.
(22) Wessling, R. A.; Oswald, J. H.; Harrison, I. R. *J. Polym. Sci., Polym. Phys. Ed.* **1973**, *11*, 875.
(23) Van Krevelen, D. W. *Properties of Polymers*, 3rd ed.; Elsevier: Amsterdam, 1990.